

PHASE EVOLUTION OF β -Al₅FeSi DURING RECYCLING Al-Si-Fe ALLOYS BY Mg MELT

*Tong Gao, Zengqiang Li, Yaoxian Zhang, Jingyu Qin, and*Xiangfa Liu

*Key Laboratory for Liquid-Solid Structural Evolution and Processing of Materials, Ministry of Education,
Shandong University, 17923 Jingshi Road, Jinan 250061, PR China*

(*Corresponding authors: tgao@sdu.edu.cn [Tong Gao]; xfliu@sdu.edu.cn [Xiangfa Liu])

ABSTRACT

The recycling of aluminum materials is a green industry while Al-Si-Fe is a typical scrap aluminum alloy. The key point of recycling Al-Si-Fe alloys is to separate Al and Fe. A method by introducing Al-Si-Fe alloy into Mg melt has been investigated in this work. A separation layer with gathered Fe-rich and Al-poor Fe₃Al_{0.7}Si_{0.3} particles were obtained at the bottom of the cooled ingot, indicating that β -Al₅FeSi phase evolves to Fe₃Al_{0.7}Si_{0.3}, and quantities of Al are released to the upper Mg matrix simultaneously. However, the evolution of Al₃Fe by adding binary Al-Fe alloy into Mg melt is different. It is supposed that element Si plays an important role in the phase evolution procedure, thus affects the performance of this method.

KEYWORDS

Al recycling, Casting, Mg melt, Phase evolution

INTRODUCTION

The rapid development of aeronautic, automotive and aerospace technologies strongly depends on the consumption of materials while sustainable development is the future direction. Aluminum is a recyclable material and Fe is one of the most common impurities. Fe can be introduced into Al alloys by adding low-purity alloying materials and by using unprotected ferrous crucible, tools, or equipment (Belov, Eskin, & Avxentieva, 2005; Lu & Dahle, 2005). For instance, wear-resistant rings are usually inserted into piston head when producing Al-Si pistons and an infiltration procedure by putting the cast iron rings into Al melt before casting is always essential. As a result, both the re-melting of pistons and the reuse of Al melt for infiltrating rings lead to the enrichment of Fe element, which can be even high to 5 wt.% (Viala, Peronnet, Barbeau, Bosselet, & Bouix, 2002).

It is widely known that coarse β -Al₃FeSi particles will form in high Fe-contained Al-Si-Fe alloys which is harmful for the mechanical properties. In the past decades, several methods to eliminate the harmful effect of β -Al₃FeSi have been investigated which can be widely referred (Munson, 1967; Lee, Kawamura, Inoue, Cho, & Masumoto, 1997; Suárez-Peña & Asensio-Lozano, 2006; Eidhed, 2008). These methods can be divided into two kinds. One is to aggregate and remove the Fe-rich phase through the methods of centrifugation, gravity filtration or magnetic separation. The other way is modifying the morphology of flake-like β -Al₃FeSi by overheating the melt or adding neutralized elements. However, these traditional methods are rarely used due to respective disadvantages, while the commonly used method in industries is using primary aluminum for dilution. However, only less than 30 wt.% of scrap Al can be added into primary Al melt for each melting work while it also results in the decrease of product quality simultaneously (Zhang, Liu, & Liu, 2016).

Based on our previous work (Gao, Li, Zhang, Qin, & Liu, 2017), a method by using Mg melt to deal with Al-6Si-4Fe alloy have been studied in this paper. Due to the evolution preference of Fe-rich phase and the density variation between it and Mg melt, the separation of Al and Fe can be achieved. The performance of this method dealing with Al-4Fe alloy was also investigated for comparison.

EXPERIMENTAL

The materials used in this study include commercial purity Mg (99.8 wt.%), commercial purity Al (99.8 wt.%), commercial purity crystalline Si (99.9 wt.%) and commercial purity Fe (99.9 wt.%). Ternary Al-12Si-4Fe and binary Al-4Fe alloys were firstly prepared by high frequency induction furnace. To check the separation performance of Al and Fe elements by this method, the experiments were carried as follows: first, Mg ingot was melted under the protection of 1% RJ-2 flux (Han, & Liu, 2016) in a BN ceramic crucible as shown in Figure 1a, by using a resistance furnace to 780 degree centigrade, *i.e.* 1053 K. Then Al-12Si-4Fe or Al-4Fe alloy was added into the melt with the proportion of 10 wt.%. After the alloy totally melted, the melt was held for 30 min and cooled in the air to room temperature. Mg-Al alloy can be obtained in the upper part of the ingot, while a deposition layer can be obtained at the bottom of the crucible, as shown in Figure 1b and 1c.

Metallographic specimens were mechanically ground and polished by using MgO turbid liquid in standard routines. The microstructure observations were carried out by a field emission scanning electron microscope (FESEM, Hitachi SU-70) operated at 15 kV and linked with an energy dispersive X-ray spectrometry (EDX) attachment. The phase identification of the samples was detected by X-ray diffraction (XRD) with a D/max-RB diffractometer (Rigaku, Tokyo, Japan) using Cu K α radiation at 40 kV and 100 mA.

The *ab initio* molecular dynamics simulation (AIMD), based on density functional theory, was used to calculate the information of clusters in Mg-Al-Fe system. The AIMD simulation was conducted using the Vienna *ab initio* simulation package (VASP) (Kresse & Furthmüller, 1996) by implementing the projector augmented-wave method (Kresse & Joubert, 1999).

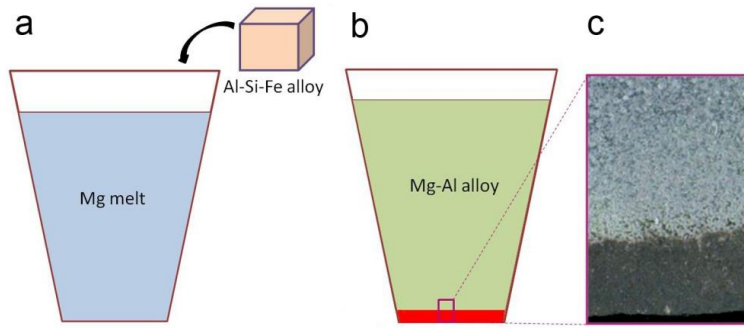


Figure 1. Schematic diagram for recycling Al–Si–Fe alloys: (a) introducing Al–Si–Fe into Mg melt; (b) after melt holding and cooling, a separation layer rich in Fe is formed; (c) image of the separation layer.

RESULTS AND DISCUSSION

Figure 2a is the microstructure of the Al–12Si–4Fe alloy. The primary Fe–rich intermetallics perform flake–like, which is the common morphology in such alloys. After the alloy was introduced into Mg melt and applied above mentioned melting and cooling procedure, a separation layer formed in the cooled Mg ingot, whose microstructure is displayed in Figure 2b. It can be found that amounts of Fe–rich particles locate densely while the size, distribution and morphology of the Fe–rich particles in the separation layer are shown in Figure 2c. The particles exhibit block–like with average size of about 5 μm , totally different from the flake–like particles (Figure 2a).

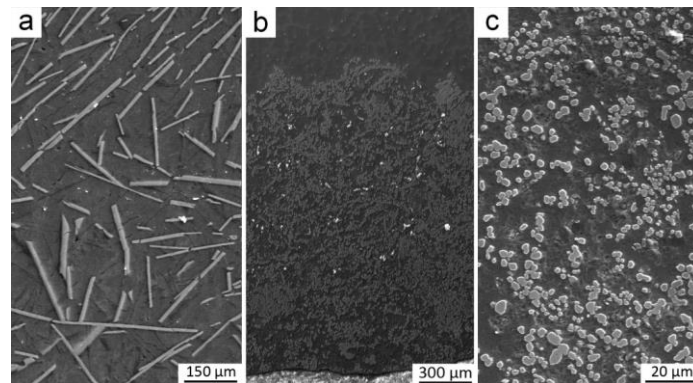


Figure 2. Microstructure of the Al–12Si–4Fe alloy (a), the formed separation layer in the cooled Mg ingot (b) and the blocky Fe–rich particles (c).

Corresponding EDX results of the Fe–rich intermetallics in Al–12Si–4Fe alloy and in the separation layer of the cooled ingot are shown in Figure 3a and b, respectively. From the detected spectrum and element contents, it can be found that the original flake–like Fe–rich phase is $\beta\text{-Al}_3\text{FeSi}$. This phase is quite rich of Al, *i.e.* a large proportion of Al is fettered by the phase and therefore cannot be efficiently recycled by using traditional methods as mentioned earlier. However, after treating by the method displayed in Figure 1, the obtained block–like Fe–rich particles have a much lower content of Al (Figure 3b). The ratio between Al and Fe has evolved from 4.65: 1 (Figure 3a) to 0.80: 1 (Figure 3b). This indicates that quantities of Al have been released to the above Mg melt and thus can be recycled through this method.

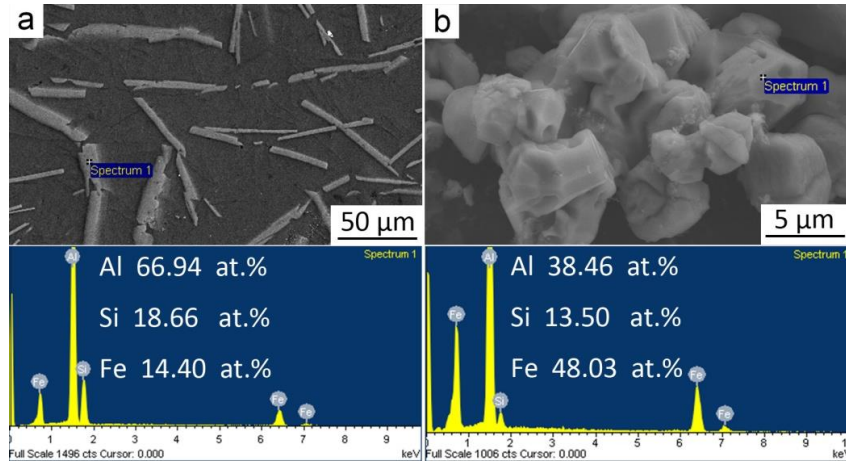


Figure 3. EDX results of the Fe-rich phase in Al-12Si-4Fe alloy (a) and in the separation layer (b).

Figure 4 is the XRD pattern of the separation layer, in which the main Fe-rich phase is detected to be $\text{Fe}_3\text{Al}_{0.7}\text{Si}_{0.3}$ (Cubic, $Fm-3m$), *i.e.* phase evolution has occurred from $\beta\text{-Al}_5\text{FeSi}$ to $\text{Fe}_3\text{Al}_{0.7}\text{Si}_{0.3}$ in Mg melt. As already discussed earlier, this phase is quite beneficial for Al recycling.

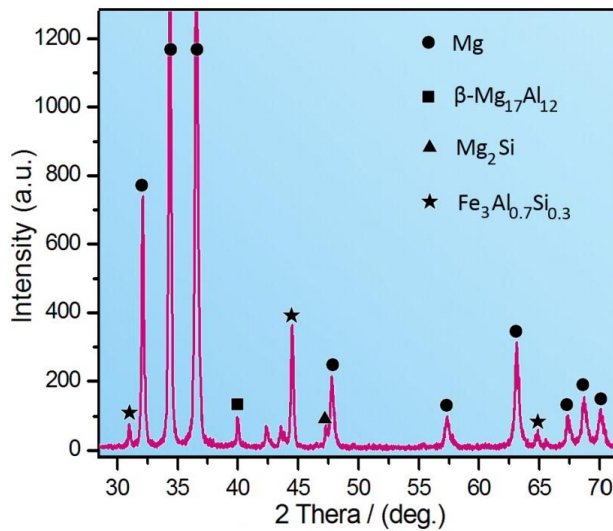


Figure 4 XRD pattern of the separation layer.

In order to acquire the detailed evolution procedure of $\beta\text{-Al}_5\text{FeSi}$ phase in Mg melt, the intermediate stage was obtained and the microstructure is shown in Figure 5a. It was found that after introducing into Mg melt, the particles evolve to polyporous while they still keep the outline of original flake-like shape. EDX result (Figure 5b) indicates that the polyporous particles are the above mentioned $\text{Fe}_3\text{Al}_{0.7}\text{Si}_{0.3}$ phase. With a longer holding process, the polyporous particles break into small blocky ones (Figure 5c). Therefore, a schematic diagram can be drawn based on the experimental results. As shown in Figure 5d, 5e and 5f, after the Al-12Si-4Fe alloy was added into Mg melt, phase structure evolution ($\beta\text{-Al}_5\text{FeSi} \rightarrow \text{Fe}_3\text{Al}_{0.7}\text{Si}_{0.3}$) and morphology evolution (flake-like \rightarrow coralline \rightarrow blocky) occurs simultaneously.

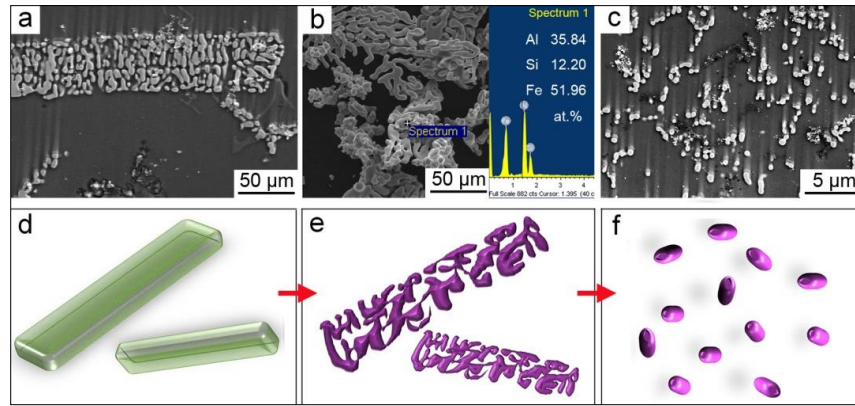


Figure 5. Microstructure and EDX of $\text{Fe}_3\text{Al}_{0.7}\text{Si}_{0.3}$ phase in the intermediate stage (a, b) and final stage (c). Schematic diagram of the evolution procedure of $\beta\text{-Al}_5\text{FeSi}$ in Mg melt (d–f).

To analyze what happened to $\beta\text{-Al}_5\text{FeSi}$ phase in Mg melt, another experiment was conducted, *i.e.* Si-free binary Al–4Fe alloy was used for comparison. The microstructure of Al–4Fe alloy is shown in Figure 6a. Similar with $\beta\text{-Al}_5\text{FeSi}$, the Fe-rich particles, *i.e.* Al_3Fe also exhibit flake-like. After introducing into Mg melt with the same melting and cooling parameters, a separation layer has also been obtained as shown in Figure 6b. It was found that the Fe-rich phase has also evolved into block-like. However, based on the EDS result (Figure 6c), the particles can still be expressed by the formula Al_3Fe . Therefore, it means that different from the evolution behavior of $\beta\text{-Al}_5\text{FeSi}$ phase in Mg melt, only morphology evolution but not phase structure evolution was detected for Si-free Al_3Fe .

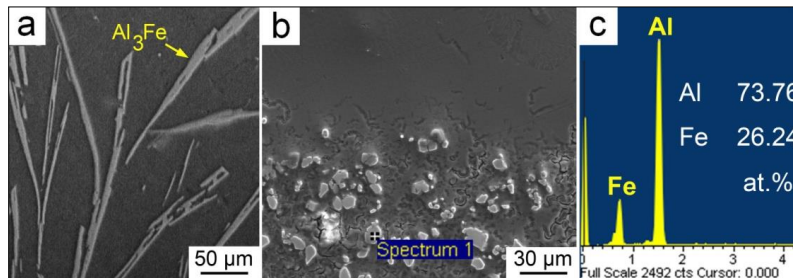


Figure 6. (a) Microstructure of binary Al–4Fe alloy; (b, c) Microstructure and EDX of the Fe-rich particles in the separation layer obtained using this method.

It is quite confused why Al_3Fe does not evolve to another Fe-rich and Al-poor phase in Mg melt, just as the performance of $\beta\text{-Al}_5\text{FeSi}$. To clarify this question, A AIMD calculation on the Mg–Al–Fe system was then conducted. Due to the amount limitation of calculation, a total number of 200 atoms were used. However, based on the experiment system (Mg+10 wt.% of Al–4Fe), the actual Fe atom number is calculated to be less than 1. This will result in quite large statistical error of the structure functions. Therefore, the system was then designed as $\text{Mg}_{177}\text{Al}_{18}\text{Fe}_5$. The obtained partial pair correlation functions at 1173K are shown in Figure 7. It is clearly observed that the first peak of partial pair correlation function $g_{\text{Al-Fe}}(r)$ curve is much higher than the other curves, indicating that the affinity of Al–Fe pairs is strongest. For the $g_{\text{Fe-Fe}}(r)$ curve, the second peak is more obvious than the first one, indicating that Fe atoms prefer to avoid meeting each other directly. Therefore, it means that it is not easy to make Fe-rich clusters evolve to a much richer one in the Mg–Al–Fe system. Also, the Fe atoms bind the Al atoms strongly in the melt, even surrounded by amounts of Mg atoms. As a result, Mg melt fails to prompt Al_3Fe phase evolve to an Al-poor phase.

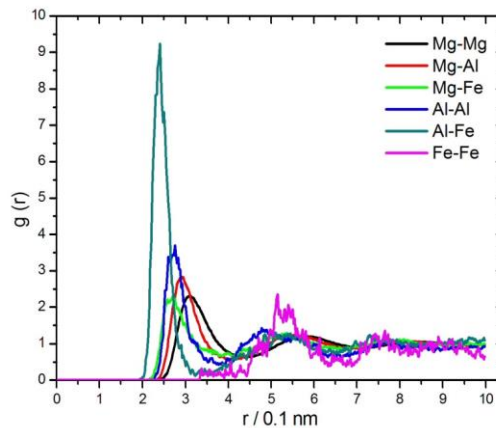


Figure 7. Partial pair correlation functions of $\text{Mg}_{177}\text{Al}_{18}\text{Fe}_5$ system at 1173K.

Based on the different behavior of $\beta\text{-Al}_5\text{FeSi}$ and Al_3Fe in Mg melt, it is reasonable to suppose that Si plays an important role in the phase evolution during recycling Al–Si–Fe alloys. It is believed that the detailed mechanism still needs further study. Besides, since the industrial scrap Al–Si–Fe alloys may have complex composition, the influence of other impurities on the performance of this method remains doubtful. Continued efforts should be made for promoting this method in industries.

CONCLUSIONS

The separation performance on Al and Fe by introducing 10 wt.% of Al–6Si–4Fe alloy into Mg melt has been discussed in this work. Along with the evolution from flake-like $\beta\text{-Al}_5\text{FeSi}$ to block-like $\text{Fe}_3\text{Al}_{0.7}\text{Si}_{0.3}$, a separation layer rich of Fe-rich particles was obtained at the bottom of the melt. Through this procedure, Al can be released to the upper melt and thus can be gathered and recycled. Compared with $\beta\text{-Al}_5\text{FeSi}$, the evolution of Al_3Fe in Mg melt is different. Only morphological evolution by not phase structure evolution was detected. It is regarded that Si plays a significant role in the evolution procedure.

ACKNOWLEDGMENTS

This research was financially supported by the National Natural Science Foundation of China (No. 51601106), the China Postdoctoral Science Foundation (No. 2017T100489), the Fundamental Research Funds of Shandong University (2016GN012) and Special Fund for Postdoctoral Innovation Project of Shandong Province (201701010).

REFERENCES

- Belov N.A., Eskin D.G., & Avxentieva N.N. (2005). Constituent phase diagrams of the Al–Cu–Fe–Mg–Ni–Si system and their application to the analysis of aluminium piston alloys, *Acta Materialia*, 53, 4709–4722. <http://dx.doi.org/10.1016/j.actamat.2005.07.003>
- Eidhed W. (2008). Modification of $\beta\text{-Al}_5\text{FeSi}$ compound in recycled Al–Si–Fe cast alloy by using Sr, Mg and Cr additions, *Journal of Materials Science & Technology*, 24, 45–47.
- Gao T., Li Z.Q., Zhang Y.X., Qin J.Y., & Liu X.F. (2017). Evolution of Fe-rich phases in Mg melt and a novel method for separating Al and Fe from Al–Si–Fe alloys, *Materials & Design*, 134, 71–80. <http://dx.doi.org/10.1016/j.matdes.2017.08.029>
- Han G., & Liu X.F. (2016). Phase control and formation mechanism of Al–Mn(–Fe) intermetallic particles

- in Mg–Al–based alloys with FeCl₃, addition or melt superheating, *Acta Materialia*, 114, 54–66. [http://dx.doi.org/ 10.1016/j.actamat.2016.05.012](http://dx.doi.org/10.1016/j.actamat.2016.05.012)
- Kresse G., & Furthmüller J. (1996). Efficiency of ab-initio total energy calculations for metals and semiconductors using a plane-wave basis set, *Computational Materials Science*, 6, 15–50. [http://dx.doi.org/ 10.1016/0927-0256\(96\)00008-0](http://dx.doi.org/10.1016/0927-0256(96)00008-0)
- Kresse G., & Joubert D. (1999). From ultrasoft pseudopotentials to the projector augmented-wave method, *Physical Review B*, 59, 1758–1775. [http://dx.doi.org/ 10.1103/PhysRevB.59.1758](http://dx.doi.org/10.1103/PhysRevB.59.1758)
- Lee T.H., Kawamura Y., Inoue A., Cho S.S., & Masumoto T. (1997). Mechanical properties of rapidly solidified Al–Si–Ni–Ce P/M alloys, *Scripta Materialia*, 36, 475–480. [http://dx.doi.org/ 10.1016/S1359-6462\(96\)00404-6](http://dx.doi.org/10.1016/S1359-6462(96)00404-6)
- Lu L., & Dahle A.K. (2005). Iron-rich intermetallic phases and their role in casting defect formation in hypoeutectic Al–Si alloys, *Metallurgical And Materials Transactions A–Physical Metallurgy And Materials Science*, 36, 819–835. [http://dx.doi.org/ 10.1007/s11661-005-1012-4](http://dx.doi.org/10.1007/s11661-005-1012-4)
- Munson D. (1967). A clarification of the phases occurring in aluminum-rich aluminum–iron–silicon alloys with particular reference to the ternary phase α -AlFeSi, *Journal of the Institute of Metals*, 95, 217–219.
- Suárez–Peña B., & Asensio–Lozano J. (2006). Influence of Sr modification and Ti grain refinement on the morphology of Fe-rich precipitates in eutectic Al–Si die cast alloys, *Scripta Materialia*, 54, 1543–1548. [http://dx.doi.org/ 10.1016/j.scriptamat.2006.01.029](http://dx.doi.org/10.1016/j.scriptamat.2006.01.029)
- Viala J.C., Peronnet M., Barbeau F., Bosselet F., & Bouix J. (2002). Interface chemistry in aluminium alloy castings reinforced with iron base inserts, *Composites Part A Applied Science & Manufacturing*, 33, 1417–1420. [http://dx.doi.org/ 10.1016/S1359-835X\(02\)00158-6](http://dx.doi.org/10.1016/S1359-835X(02)00158-6)
- Zhang Y.X., Liu W.C., & Liu X.F. (2016). Segregation behavior and evolution mechanism of iron-rich phases in molten magnesium alloys, *Journal of Materials Science & Technology*, 32, 48–53. [http://dx.doi.org/ 10.1016/j.jmst.2015.10.013](http://dx.doi.org/10.1016/j.jmst.2015.10.013)